

February 29, 2020

Dear AMT Editor:

Re: Response to Reviewers' Comments from the Public Discussion - MS No.: amt-2019-393

We thank the comments by the Referee No.3 and No.4 from the public discussion. Our responses are provided below.

Comment 1 from Referee No. 3	Lines 147-150, the authors stated that random search is more efficient, which is also a unique part of this study. Please explain why it is more efficient than manual or grid search in principle and if possible, give some quantitative information																				
Author's response	<p>The grid search can be considered as an automated manual search. Grid search method and manual search method consider every combination of all the hyperparameters to build the learning models and each model needs to be evaluated to find out the one of the highest accuracies for training and prediction. For the XGBoost algorithm used in the manuscript Section 2.3.2, we tuned 7 hyperparameters. Each hyperparameter has 20 difference parameters. The grid looks like the following table:</p> <table><tr><td>Hyperparameter</td><td>P1</td><td>...</td><td>P20</td></tr><tr><td>H1</td><td></td><td></td><td></td></tr><tr><td>H2</td><td></td><td></td><td></td></tr><tr><td>...</td><td></td><td></td><td></td></tr><tr><td>H7</td><td></td><td></td><td></td></tr></table> <p>The complete grid search requires $20^7 = 1,280$ millions of trials. In this study, we used 10-fold cross validation, which means each trial will run 10 times. So, the total runs will be $1,280 \text{ millions} * 10 =$ over 12 billion, which is computationally expensive.</p> <p>For random search, instead of computing the cases of all possible combinations, random combinations of hyperparameters are selected at each trial. Due to the random nature of sampling, the entire space of the grid could be reached (Zheng 2015).</p> <p>The higher efficiency of random search can be explained by probability theory: Considering a sample space with a finite</p>	Hyperparameter	P1	...	P20	H1				H2				...				H7			
Hyperparameter	P1	...	P20																		
H1																					
H2																					
...																					
H7																					

	<p>maximum, if we need to find a sample that is within the top 5% of all the samples, 60 random observations would give us 95% probability to find the sample. The value of 60 is calculated as follows:</p> <p>As there are 5% eligible samples in the space, each random observation has 5% of chance to find the eligible sample. On another hand, each random observation has (1-5%) chance not to find the eligible sample. If we take n random observations, the chance of not to get the eligible sample would be $(1-0.05)^n$, or the chance of getting the eligible sample would be $1-(1-0.05)^n$. Let</p> $1-(1-0.05)^n > 95\%$ <p>And we can solve for $n = 60$</p> <p>Therefore, random search method would significantly save computation resource but still have a good chance to guess the close-to-optimal combination of hyperparameters.</p>
Author's changes in manuscript	<p>We added a reference below in line 150 to explain the rationale of random search method.</p> <p>Zheng (2015) explained that random search with 60 samples will find a close-to-optimal combination with 95% of probability.</p>

Comment 2 from Referee No. 3	Figure 1, I would appreciate a geographical map showing where is the monitoring location.
Author's response	a geographical map is added as Figure 2
Author's changes in manuscript	Added a new figure - Figure 2.

Comment 3 from Referee No. 3	CRAZ also monitors NOx, NMHC, ozone, and wind data, which may also influence the PM concentration. Why these data were not included in the machine learning?
Author's response	<p>The low-cost sensor evaluated in this study only measured temperature (T) and relative humidity (RH). The ultimate goal of low-cost sensor application is to provide same quality data as the reference method using available information provided by the low-cost sensor. Therefore, we only used the parameters that the sensor measured.</p> <p>Next phase of the study would be testing other types of low-cost sensors, which may provide other parameters than T and RH. In that case, we would include those parameters in machine learning.</p>

Author's changes in manuscript	Not applicable.
--------------------------------	-----------------

Comment 4 from Referee No. 3	Line 195: there is a typo: "SHAPR" should be "SHARP".
Author's response	Corrected
Author's changes in manuscript	Corrected to SHARP

Comment 5 from Referee No. 3	SHARP was used as the reference method for PM monitoring. How often was SHARP calibrated to ensure its data quality
Author's response	The SHARP instrument is regulated by the provincial air monitoring directive. It was calibrated monthly.
Author's changes in manuscript	We added a clarification in Line 171 The instrument was calibrated monthly

Comment 6 from Referee No. 3	Line 228: how the hyperparameters were determined?
Author's response	The hyperparameters were determined by the XGBoost algorithm itself. Detailed explanation of each hyperparameter is provided in the XGBoost documentation https://xgboost.readthedocs.io/en/latest/parameter.html
Author's changes in manuscript	We added the following reference in line 238 Detailed explanation of each hyperparameter is provided in the XGBoost documentation (XGBoost developers, 2019)

Comment 7 from Referee No. 3	Figure 3: will you explain what the shape of erlenmeyer flask means in the plot?
Author's response	The plots outside of the boxplots in Figure 3 is called violin plot. The violin plot is to describe the density of data. More details can be found in the following link:

	https://mode.com/blog/violin-plot-examples/
Author's changes in manuscript	<p>The following sentences were added in Line 264</p> <p>The violin plot in Figure 3 describes the distribution of the PM2.5 values measured by the low-cost sensor and SHARP using density curve. The width of each curve represents the frequency of PM2.5 values at each concentration level.</p>

Comment 8 from Referee No. 3	One aspect of the uniqueness of this study is that its study covers different seasons. I would like to see a brief discussion how season influence the results of low-cost sensors.
Author's response	<p>We added a section to discuss the seasonal impact in Section 3.5.2</p> <p>We assessed the seasonal impact on the low-cost sensor by comparing the mean of absolute differences between the daily average of sensor values and the daily average of SHARP values in winter (December 2018 to February 2019) and spring (March 2019 to April 2019). A descriptive statistic is presented in Table 7.</p> <p>We used a two-sample t test to assess if the means of absolute differences for winter and spring were equal. The p value of the t test was 0.754. Because $P = 0.754 > \alpha = 0.05$, we retained the null hypothesis. There was not sufficient evidence at the $\alpha = 0.05$ level to conclude that the means of absolute differences between the low-cost sensor and SHARP PM values were significantly different for winter season and spring season.</p>
Author's changes in manuscript	Added a section 3.5.2

Comment 1 from Referee No. 4	Work with sensor vendor to find out the reason of high equipment disability rate and build a larger sensor network in an area to evaluate the calibration method crossing different sensors
Author's response	<p>We thank the reviewers' recommendation for our future work. We think it might be caused by water damage to the controller board.</p> <p>We planned to carry out a Phase 2 of the study to work with the sensor vendors or may try different sensors to understand what might be the cause that sensors do not last long.</p> <p>In phase 2, we also plan to deploy multiple sensors at multiple Alberta air monitoring stations for a longer time, such as 1 year, so</p>

	we can test sensor precision and bias, as well as transferability of machine learning models.
Author's changes in manuscript	Not applicable

Comment 2 from Referee No. 4	Expand the temperature range to a warm condition, such as 30 C- 38 C to evaluation RH with higher temperature's effect on low cost sensor and calibration method
Author's response	<p>We thank the reviewers' recommendation for our future work.</p> <p>Because of sensor failure, the sensor we used did not last to summer. We plan to set up experiments in phase 2 to cover a boarder ranges of weather condition</p> <p>We added a short discussion about season impacts.</p> <p>We assessed the seasonal impact on the low-cost sensor by comparing the mean of absolute differences between the daily average of sensor values and the daily average of SHARP values in winter (December 2018 to February 2019) and spring (March 2019 to April 2019). A descriptive statistic is presented in Table 7.</p> <p>We used a two-sample t test to assess if the means of absolute differences for winter and spring were equal. The p value of the t test was 0.754. Because $P = 0.754 > \alpha = 0.05$, we retained the null hypothesis. There was not sufficient evidence at the $\alpha = 0.05$ level to conclude that the means of absolute differences between the low-cost sensor and SHARP PM values were significantly different for winter season and spring season.</p>
Author's changes in manuscript	Added a section 3.5.2

Respectful submitted
Calgary, Alberta Canada

Si et al.

Evaluation and Calibration of a Low-cost Particle Sensor in Ambient Conditions Using Machine Learning ~~Technologies~~ Methods

Minxing Si^{1,2,a}, Xiong Ying^{1,a}, Shan Du³, Ke Du^{1*}

¹Department of Mechanical and Manufacturing Engineering, University of Calgary, 2500 University Drive. NW, Calgary, AB, Canada, T2N 1N4

²Tetra Tech Canada Inc., 140 Quarry Park Blvd, Calgary AB Canada, T2C 3G3

³Department of Computer Science, Lakehead University, 955 Oliver Road, Thunder Bay, ON, Canada, P7B 5E1

*Correspondence to Ke Du (kddu@ucalgary.ca)

^a The authors contributed equally to the work.

Abstract. Particle sensing technology has shown great potential for monitoring particulate matter (PM) with very few temporal and spatial restrictions because of low-cost, compact size, and easy operation. However, the performance of low-cost sensors for PM monitoring in ambient conditions has not been thoroughly evaluated. Monitoring results by low-cost sensors are often questionable. In this study, a low-cost fine particle monitor (Plantower PMS 5003) was co-located with a reference instrument, named Synchronized Hybrid Ambient Real-time Particulate (SHARP) monitor, in Calgary Varsity air monitoring station from December 2018 to April 2019. The study evaluated the performance of this low-cost PM sensor in ambient conditions and calibrated its readings using simple linear regression (SLR), multiple linear regression (MLR), and two more powerful machine learning algorithms using random search techniques for the best model architectures. The two machine learning algorithms are XGBoost and feedforward neural network (NN). Field evaluation showed that the Pearson r between the low-cost sensor and the SHARP instrument was 0.78. Fligner and Killeen (F-K) test indicated a statistically significant difference between the variances of the $PM_{2.5}$ values by the low-cost sensor and by the SHARP instrument. Large overestimations by the low-cost sensor before calibration were observed in the field and were believed to be caused by the variation of ambient relative humidity. The root mean square error (RMSE) was 9.93 when comparing the low-cost sensor with the SHARP instrument. The calibration by the feedforward NN had the smallest RMSE of 3.91 in the test dataset, compared to the calibrations by SLR (4.91), MLR (4.65), and XGBoost (4.19). After calibrations, the F-K test using the test dataset showed that the variances of the $PM_{2.5}$ values by the NN and the XGBoost and by the reference method were not statistically significantly different. From this study, we conclude that feedforward NN is a promising method to address the poor performance of the low-cost sensors for $PM_{2.5}$ monitoring. In addition, the random search method for hyperparameters was demonstrated to be an efficient approach for selecting the best model structure.

Keywords: Low-cost sensor, machine learning, TensorFlow, XGBoost, $PM_{2.5}$

32 **1 Introduction**

33 Particular matter (PM), whether it is natural or anthropogenic, has pronounced effects on human health, visibility, and global
34 climate (Charlson et al., 1992; Seinfeld and Pandis, 1998). To minimize the harmful effects of PM pollution, the
35 Government of Canada launched the National Air Pollution Surveillance (NAPS) program in 1969 to monitor and regulate
36 PM and other criteria air pollutants in populated regions, including ozone (O₃), sulfur dioxide (SO₂), carbon monoxide (CO),
37 nitrogen dioxide (NO₂). Currently, PM monitoring is routinely carried out at 286 designated air sampling stations in 203
38 communities in all provinces and territories of Canada (Government of Canada, 2019). Many of the monitoring stations use
39 Beta Attenuation Monitor (BAM), which is based on the adsorption of beta radiation, or Tapered Element Oscillating
40 Microbalance (TEOM) instrument, which is a mass-based technology to measure PM concentrations. An instrument that
41 combines two or more technologies, such as Synchronized Hybrid Ambient Real-time (SHARP), is also used in some
42 monitoring stations. The SHARP instrument combines light scattering with beta attenuation technologies to determine PM
43 concentrations.

44 Although these instruments are believed to be accurate for measuring PM concentration and have been widely used by
45 many air monitoring stations worldwide (Chow and Watson, 1998; Patashnick and Rupprecht, 1991), they have common
46 drawbacks: they can be challenging to operate, bulky, and expensive. The instrument costs from 8,000 Canadian dollars
47 (CAD) to tens of thousands of dollars (Chong and Kumar, 2003). The SHARP instrument used in this study as a reference
48 method costs approximately \$40,000 (CDNova Instrument Ltd., 2017). Significant resources, such as specialized personnel
49 or technicians, are also required for regular system calibration and maintenance. In addition, the sparsely spread stations may
50 only represent PM levels in limited areas near the stations because PM concentrations vary spatially and temporally
51 depending on local emission sources as well as meteorological conditions (Xiong et al., 2017). Such a low-resolution PM
52 monitoring network cannot support public exposure and health effects studies that are related to PM, because these studies
53 require high spatial- and temporal-resolution of monitoring network in the community (Snyder et al., 2013). In addition, the
54 well-characterized scientific PM monitors are not portable due to their large size and volumetric flow rate, which means they
55 are not practical for measuring personal PM exposure (White et al., 2012).

56 As a possible solution to the above problems, a large number of low-cost PM sensors could be deployed, and a high-
57 resolution PM monitoring network could be constructed. Low-cost PM sensors are portable and commercially available.
58 They are cost-effective and easy to deploy, operate, and maintain, which offers significant advantages compared to
59 conventional analytical instruments. If many low-cost sensors are deployed, PM concentrations can be monitored
60 continuously and simultaneously at multiple locations for a reasonable cost (Holstius et al., 2014). A dense monitoring
61 network using low-cost sensors can also assist in mapping hotspots of air pollution, creating emission inventories of air
62 pollutants, and estimating adverse health effects due to personal exposure to the PM (Kumar et al., 2015).

Field Code Changed

Field Code Changed

Field Code Changed

Field Code Changed

Field Code Changed

Field Code Changed

Field Code Changed

Field Code Changed

Field Code Changed

63 However, low-cost sensors present challenges for broad application and installation. Most sensor systems have not been
 64 thoroughly evaluated (Williams et al., 2014), and the data generated by these sensors are of questionable quality (Wang et
 65 al., 2015). Currently, most low-cost sensors are based on laser light scattering technology (LLS), and the accuracy of LLS is
 66 mostly affected by particle composition, size distribution, shape, temperature, and relative humidity (Jayaratne et al., 2018;
 67 Wang et al., 2015).

68 Several studies evaluated LLS sensors by comparing the performance of low-cost sensors with medium- to high-cost
 69 instruments under laboratory and ambient conditions. For example, Zikova et al. (2017) used low-cost Speck monitors to
 70 measure PM_{2.5} concentrations in indoor and outdoor environments, and the low-cost sensors overestimated the concentration
 71 by 200% for indoor and 500% for outdoor, compared to a reference instrument – Grimm 1.109 dust monitor. Jayaratne et al.
 72 (2018) reported that PM₁₀ concentrations generated by a Plantower low-cost particle sensor (PMS 1003) were 46% greater
 73 than a TSI 8350 DustTrak DRX aerosol monitor under a foggy environment. Wang et al. (2015) compared PM
 74 measurements from three low-cost LLS sensors – Shinyei PPD42NS, Samyoung DSM501A, and Sharp GP2Y1010AU0F –
 75 with a SidePack (TSI Inc.) using smoke from burning incense. High linearity was found with R² greater than 0.89, but the
 76 responses depended on particle composition, size, and humidity. Air Quality Sensor Performance Evaluation Center (AQ-
 77 SPEC) of South Coast Air Quality Management District (SCAQMD) also evaluated the performances of three Purple Air
 78 PA-II sensors (model: Plantower PMS 5003) by comparing their readings with two United States Environmental Protection
 79 Agency (US EPA) Federal Equivalent Method (FEM) instruments – BAM (MetOne) and Grimm dust monitors in laboratory
 80 and field environments in south California (Papapostolou et al., 2017). Overall, the three sensors showed moderate to good
 81 accuracy, compared to the reference instrument for PM_{2.5} for a concentration range between 0 to 250 µg m⁻³. Lewis et al.
 82 (2016) evaluated low-cost sensors in the field for O₃, nitrogen oxide (NO), NO₂, volatile organic compounds (VOCs), PM_{2.5},
 83 and PM₁₀; only O₃ sensors showed good performance compared to the reference measurements.

84 Several studies developed calibration models using multiple techniques to improve low-cost sensors' performance. For
 85 example, De Vito et al. (2008) tested feedforward neural network (NN) calibration for benzene monitoring and reported a
 86 further calibration was needed for low concentrations. Bayesian optimization was also used to search feedforward NN
 87 structures for the calibrations of CO, NO₂, and NO_x low-cost sensors (De Vito et al., 2009). Zheng et al. (2018) calibrated
 88 Plantower low-cost particle sensor PMS 3003 by fitting a linear least-squares regression model. A nonlinear response was
 89 observed when ambient PM_{2.5} exceeded 125 µg m⁻³. The study concluded that a quadratic fit was more appropriate than a
 90 linear model to capture this nonlinearity.

91 Zimmerman et al. (2018) explored three different calibration models, including laboratory univariate linear regression,
 92 empirical MLR, and a more modern machine learning algorithm, random forests (RF), to improve Real-time Affordable
 93 Multiple-Pollutant (RAMP) sensor's performance. They found that the sensors calibrated by RF models improved their
 94 accuracy and precision over time, with average relative errors of 14% for CO, 2% for CO₂, 29% for NO₂, and 15% for O₃.

Field Code Changed

Field Code Changed

Field Code Changed

Field Code Changed

Field Code Changed

Field Code Changed

Field Code Changed

Field Code Changed

Field Code Changed

Field Code Changed

Field Code Changed

Field Code Changed

95 The study concluded that combining RF models with low-cost sensors is a promising approach to address the poor
96 performance of low-cost air quality sensors.

97 Spinelle et al. (2015) reported several calibration methods for low-cost O₃ and NO₂ sensors. The best calibration method
98 for NO₂ was an NN algorithm with feedforward architecture. O₃ could be calibrated by simple linear regression (SLR).
99 Spinelle et al. (2017) also evaluated and calibrated NO, CO, and CO₂ sensors, and the calibrations by feedforward NN
100 architectures showed the best results. Similarly, Cordero et al. (2018) performed a two-step calibration for an AQmesh NO₂
101 sensor using supervised machine learning regression algorithms, including NNs, RFs, and Support Vector Machines
102 (SVMs). The first step produced an explanatory variable using multivariate linear regression. In the second step, the
103 explanatory variable was fed into machine learning algorithms, including RF, SVM, and NN. After the calibration, the
104 AQmesh NO₂ sensor met the standards of accuracy for high concentrations of NO₂ in the European Union's Directive
105 2008/50/EC on Air Quality. They highlighted the need to develop an advanced calibration model, especially for each sensor,
106 as the responses of individual sensors are unique.

107 Williams et al. (2014) evaluated eight low-cost PM sensors; the study showed frequent disagreement between the low-
108 cost PM sensors and FEMs. In addition, the study concluded that the performances of the low-cost sensors were significantly
109 impacted by temperature and relative humidity (RH). Recurrent NN architectures were also tested for the calibrations of
110 some gas sensors (De Vito et al., 2018; Esposito et al., 2016). The results showed that the dynamic approaches performed
111 better than traditional static calibration approaches. Calibrations of PM_{2.5} sensors were also reported in recent studies. Lin et
112 al. (2018) performed two-step calibrations for PM_{2.5} sensors using 236 hourly data collected on buses and road cleaning
113 vehicles. The first step was to construct a linear model, and the second step used RF machine learning for further calibration.
114 The RMSE after the calibrations was 14.76 µg m⁻³, compared to a reference method. The reference method used in this study
115 was a Dylos DC11700 device, which is not a US EPA federal reference method (FRM) or FEM. Loh and Choi (2019) trained
116 and tested SVC, k-nearest neighbor, RF, and XGBoost machine learning algorithms to calibrate PM_{2.5} sensors using 319
117 hourly data. XGBoost archived the best performance with a RMSE of 5.0 µg m⁻³. However, the low-cost sensors in this
118 study were not co-located with the reference method, and the machine learning models were not tested using unseen data
119 (test data) for predictive power and overfitting.

120 Although there are studies in calibrating low-cost sensors, most of them focused on gas sensors or used short-term data to
121 calibrate PM sensors. To our best knowledge, no one has reported studies on PM sensor calibration using random search
122 techniques for the best machine learning model's configuration under ambient conditions during different seasons. In this
123 study, a low-cost fine particle monitor (Plantower PMS 5003) was co-located with a SHARP monitor Model 5030 at Calgary
124 Varsity Air Monitoring Station in an outdoor environment from December 7, 2018, to April 26, 2019. The SHARP
125 instrument is the reference method in this study and is a US EPA FEM (US EPA, 2016). The objectives of this study are:
126 (1) to evaluate the performance of the low-cost PM sensor in a range of outdoor environmental conditions by comparing its

Field Code Changed

Field Code Changed

Field Code Changed

Field Code Changed

Field Code Changed

Field Code Changed

Field Code Changed

Field Code Changed

127 $PM_{2.5}$ readings with those obtained from the SHARP instrument; and (2) to assess four calibration methods: a) a SLR or
128 univariate linear regression based on the low-cost sensor values; b) a multiple linear regression (MLR) using the $PM_{2.5}$, RH,
129 and temperature measured by the low-cost sensor as predictors; c) a decision-tree-based ensemble algorithm, called
130 XGBoost or Extreme Gradient Boosting; and d) a feedforward NN architecture with a backpropagation algorithm.

131 XGBoost and NN are the most popular algorithms used on Kaggle – a platform for data science and machine learning
132 competition. In 2015, 17 winners out of 29 competitions on Kaggle used XGBoost, 11 winners used deep NN algorithm
133 (Chen and Guestrin, 2016).

Field Code Changed

134 This study is unique in the following ways:

135 1) To the best of our knowledge, this is the first comprehensive study using long-term data to calibrate low-cost
136 particle sensors in the field. Most previous studies focused on calibrating gas sensors (Maag et al., 2018). There are
137 two studies on PM sensor calibrations using machine learning, but they used a short-term dataset that did not
138 include seasonal changes in ambient conditions (Lin et al., 2018; Loh and Choi, 2019). The shortcomings of the two
139 studies were discussed above.

Field Code Changed

Field Code Changed

140 2) Although several studies researched the calibration of gas sensors using NN, this study explores multiple
141 hyperparameters to search for the best NN architecture. Previous research configured one to three hyperparameters,
142 compared to six in this study (De Vito et al., 2008, 2009, 2018; Esposito et al., 2016; Spinelle et al., 2015, 2017). In
143 addition, this study tested the Rectified Linear Unit (ReLU) as the activation function in the feedforward NN.
144 Compared to sigmoid and tanh activation functions used in the previous studies for NN calibration models, the
145 ReLU function can accelerate the convergence of stochastic gradient descent to a factor of 6 (Krizhevsky et al.,
146 2017).

Field Code Changed

Field Code Changed

147 3) Previous NN and tree-based calibration models used manual search or grid search for hyperparameters tuning. This
148 study introduced random search method for the best calibration models. Random search is more efficient than
149 traditional manual and grid search (Bergstra and Bengio, 2012) and evaluates more of the search space, especially
150 when search space is more than three dimensions (Timbers, 2017). Zheng (2015) explained that random search with
151 60 samples will find a close-to-optimal combination with 95% of probability.

Field Code Changed

Field Code Changed

152 2 Method

153 2.1 Data preparation

154 One low-cost sensor unit was provided by Calgary-based company SensorUp and deployed at the Varsity station in the
155 Calgary Reginal Airshed Zone (CRAZ) in Calgary, Alberta, Canada. The unit contains one sensor, one electrical board, and
156 one housing as a shelter. The sensor in the unit is Plantower PMS 5003, and it measured outdoor fine particle ($PM_{2.5}$)

157 concentrations ($\mu\text{g m}^{-3}$), air temperature ($^{\circ}\text{C}$), and RH (%) every six seconds. The minimum detectable particle diameter by
158 the sensor is $0.3\ \mu\text{m}$. The instrument costs approximately \$20 CAD and is referred to as the low-cost sensor in this paper.

159 The low-cost sensor is based on LLS technology; $\text{PM}_{2.5}$ mass concentration is estimated from the detected amount of
160 scattered light. The LLS sensor is installed on the electrical board and then placed in the shelter for outdoor monitoring. The
161 unit has a wireless link to a router in the Varsity station. A picture of the low-cost sensor and the monitoring environment
162 where the low-cost sensor unit and the SHARP instrument were co-located is provided in Fig. 1. [The location of the Varsity](#)
163 [station is provided in Fig. 2](#). The router uses cellular service to transfer the data from the low-cost sensor to SensorUp's
164 cloud data storage system. The measured outdoor $\text{PM}_{2.5}$, temperature, and RH data at a six-second interval from 00:00 on
165 December 7, 2018, to 23:00 on April 26, 2019, were downloaded from the cloud data storage system for evaluation and
166 calibration.



167
168 **Figure 1:** The low-cost sensor used in the study and the ambient inlet of the reference method – SHARP Model 5030

169
170

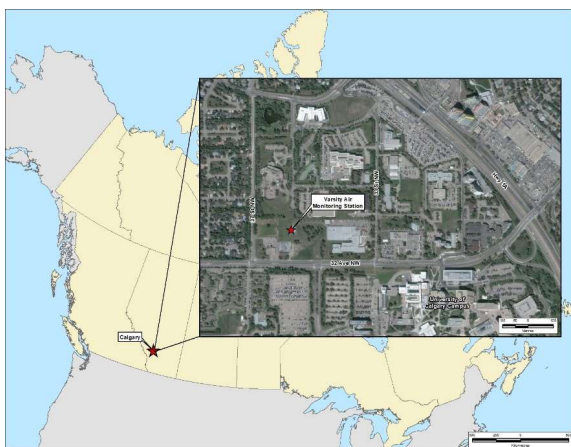


Figure 2: Location of Varsity Air Monitoring Station

Formatted: Caption

The reference instrument used to evaluate the low-cost sensor is a Thermal Fisher Scientific's SHARP Model 5030. The SHARP instrument was installed at the Calgary Varsity station by CRAZ. The SHARP instrument continuously uses two compatible technologies, light scattering and beta attenuation, to measure $PM_{2.5}$ every six minutes with an accuracy of $\pm 5\%$. The SHARP instrument is operated and maintained by CRAZ in accordance with the provincial government's guideline outlined in Alberta's air monitoring directive. The instrument was calibrated monthly. Hourly $PM_{2.5}$ data are published on the Alberta Air Data Warehouse website (<http://www.airdata.alberta.ca/>). The Calgary Varsity station also continuously monitors CO, methane, oxides of nitrogen, non-methane hydrocarbons, outdoor air temperature, O_3 , RH, total hydrocarbon, wind direction, and wind speed. Detailed information on the analytical systems for the CRAZ Varsity station can be found on their website (<https://craz.ca/monitoring/info-calgary-nw/>).

The ambient conditions in this study measured by the SHARP instrument are presented in Table 1.

Table 1: Ambient Condition Measured by SHARP

Climate Data	SHARP Value
Temperature	-31.4 °C ~ 19 °C
RH	10% ~ 99%
Wind Speed	4.3 ~ 37.1 km/h 10 m

185
186 The following steps were taken to process the raw data from 00:00 on December 7, 2018, to 23:00 on April 26, 2019:
187 1) The six-second interval data recorded by the low-cost sensor, including $PM_{2.5}$, temperature, and RH, were averaged
188 into hourly data to pair with SHARP data because only hourly SHARP data are publicly available.
189 2) The hourly sensor data and hourly SHARP data were combined into one structured data table. $PM_{2.5}$, temperature,
190 and RH by the low-cost sensor as well as $PM_{2.5}$ by SHARP columns in the data table were selected. The data table
191 then contains 3,384 rows and four columns. Each row represents one hourly data point. The columns include the data
192 measured by the low-cost sensor and the SHARP instrument.
193 3) Rows in the data table with missing values were removed – 299 missing values for $PM_{2.5}$ from the low-cost sensor
194 and 36 missing values for $PM_{2.5}$ from the SHARP instrument. The reason for missing data from the SHARP
195 instrument is because of the calibration. However, the reason for missing data from the low-cost sensor is unknown.
196 4) The data used for NN were transformed by z standardization with a mean of zero and a standard deviation of one.
197 After the above steps, the processed data table with 3,050 rows and four columns was used for evaluation and calibration.
198 The data file is provided in the supplementary information of this paper. Each row represents one example or sample for the
199 training or testing by the calibration methods.

200 **2.2 Low-cost sensor evaluation**

201 Pearson correlation coefficient was used to compare the correlation for $PM_{2.5}$ values between the low-cost sensor and the
202 SHARP. SHARP was the reference method. The $PM_{2.5}$ data by the low-cost sensor and SHARP were also compared using
203 root mean square error (RMSE), mean square error (MSE), and mean absolute error (MAE).
204 Fligner and Killeen test (F-K test) was used to evaluate the equality (homogeneity) of variances for $PM_{2.5}$ values between
205 the low-cost sensor and the SHARP instrument (Fligner and Killeen, 1976). F-K test is a superior option in terms of
206 robustness and power when data are non-normally distributed, the population means are unknown, or outliers cannot be
207 removed (Conover et al., 1981; de Smith, 2018). The null hypothesis of the F-K test is that all populations' variances are
208 equal; the alternative hypothesis is that the variances are statistically significantly different.

209 **2.3 Calibration**

210 Four calibration methods were evaluated: SLR, MLR, XGBoost, and NN. Some predictions from the SLR, MLR, and
211 XGBoost have negative values because they extrapolate observed values and regression is unbounded. When the predicted
212 $PM_{2.5}$ values generated by these calibration methods were negative, the negative values were replaced with the sensor data.
213 MLR, XGBoost, and feedforward NN use the $PM_{2.5}$, temperature, and RH data measured by the low-cost sensor as
214 inputs. The $PM_{2.5}$ measured by the SHARP instrument is used as the target to supervise the machine learning process. The

Field Code Changed

Field Code Changed

215 processed dataset with 3,050 rows and four columns was randomly shuffled and then divided into a training set, which was
216 the data used to build models and minimize the loss function, and a test set, which was the data that the model has never run
217 with before testing (Si et al., 2019). The test dataset was only used once and gave an unbiased evaluation of the final model's
218 performance. The evaluation was to test the ability of the machine learning model to provide sensible predictions with new
219 inputs (LeCun et al., 2015). The training dataset had 2,440 examples (samples). The test dataset had 610 examples (samples).

Field Code Changed

Field Code Changed

220 **2.3.1 Simple linear regression and multiple linear regression**

221 The calibration by a SLR used Equation 1.

222
$$\hat{y} = \beta_0 + \beta_1 \times \llbracket PM \rrbracket_{2.5}$$

223
$$(1)$$

224 β_0 and β_1 are the model coefficient and were calculated using the training dataset. \hat{y} is model predicted (calibrated) values.

225 $PM_{2.5}$ is the value measured by the low-cost sensor.

226 The MLR used $PM_{2.5}$, RH, and temperature measured by the low-cost sensor as predictors because the low-cost sensor
227 only measured these parameters. The model is expressed as Equation 2.

228
$$\hat{y} = \beta_0 + \beta_1 \times PM_{2.5} + \beta_2 \times T + \beta_3 \times RH \quad (2)$$

229 The model coefficients, β_0 to β_3 , were calculated using the training dataset with SHARP provided readings as \hat{y} . The
230 outputs of the models generated by the SLR and MLR were evaluated by comparing to the SHARP's readings in the test
231 dataset.

232 **2.3.2 XGBoost**

233 XGBoost is a scalable decision tree-based ensemble algorithm, and it uses a gradient boosting framework (Chen and
234 Guestrin, 2016). The XGBoost was implemented using the XGBoost (Version 0.90) and sklearn (Version 0.21.2) packages
235 in Python (Version 3.7.3). Random search method (Bergstra and Bengio, 2012) was used to tune the hyperparameters in the
236 XGBoost algorithm, and the hyperparameters tuned include

Field Code Changed

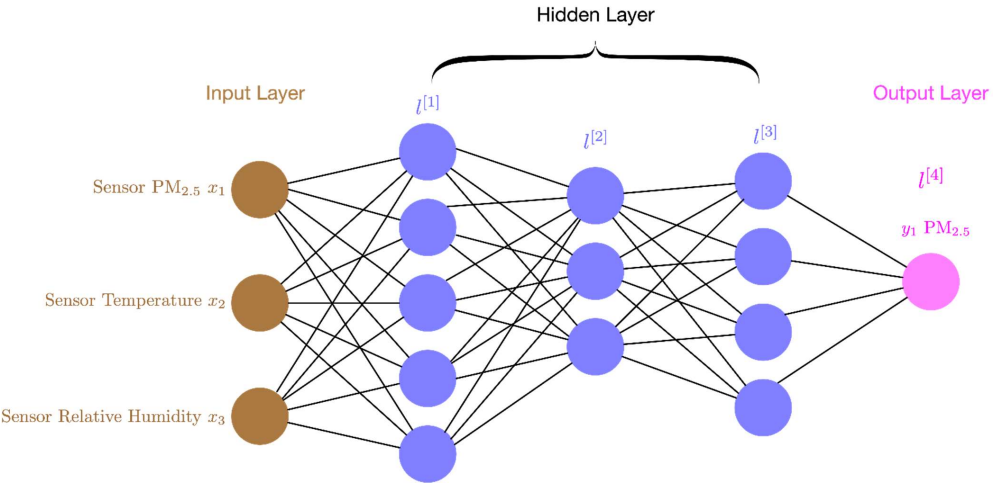
Field Code Changed

- 237 • Number of trees to fit (n_estimator)
- 238 • Maximum depth of a tree (max_depth)
- 239 • Step size shrinkage used in update (learning_rate)
- 240 • Subsample ratio of columns when constructing each tree (colsample_bytree)
- 241 • Minimum loss reduction required to make a further partition on a leaf node of the tree (gamma)
- 242 • L2 regularization on weights (reg_lambda)
- 243 • Minimum sum of instance weight needed in a child (min_child_weight)

244 [Detailed explanation of each hyperparameter is provided in the XGBoost documentation \(XGBoost developers, 2019\).](#)
 245 Ten-fold cross-validation was used to select the best model with minimum MSE from the random search. The best model
 246 was then evaluated against the SHARP PM_{2.5} data using the test dataset.

247 **2.3.3 Neural network**

248 A fully connected feedforward NN architecture was used in the study. In a fully connected NN, each unit (node) in a
 249 layer is connected to each unit in the following layer. Data from the input layer are passed through the network until the
 250 unit(s) in the output layer is (are) reached. An example of a fully connected feedforward NN is presented in Fig. 32. A
 251 backpropagation algorithm is used to minimize the difference between the SHARP measured values and the predicted values
 252 (Rumelhart et al., 1986).



253
 254 **Figure 32:** Example of a Neural Network Structure

255 The NN was implemented using the Keras (Version 2.2.4) and TensorFlow (Version 1.14.0) libraries in Python (Version
 256 3.7.3). Keras and TensorFlow were the most referenced deep learning framework in scientific research in 2017 (RStudio,
 257 2018). Keras is the front end of TensorFlow.
 258 Learning rate, L2 regularization rate, numbers of hidden layers, number of units in the hidden layers, and optimization
 259 methods were tuned using random search method provided in the scikit-learn machine learning library. Ten-fold cross-
 260 validation was used to evaluate the models. The model with the minimum MSE was considered to be the best-fit model and
 261 then used for model testing.

Field Code Changed

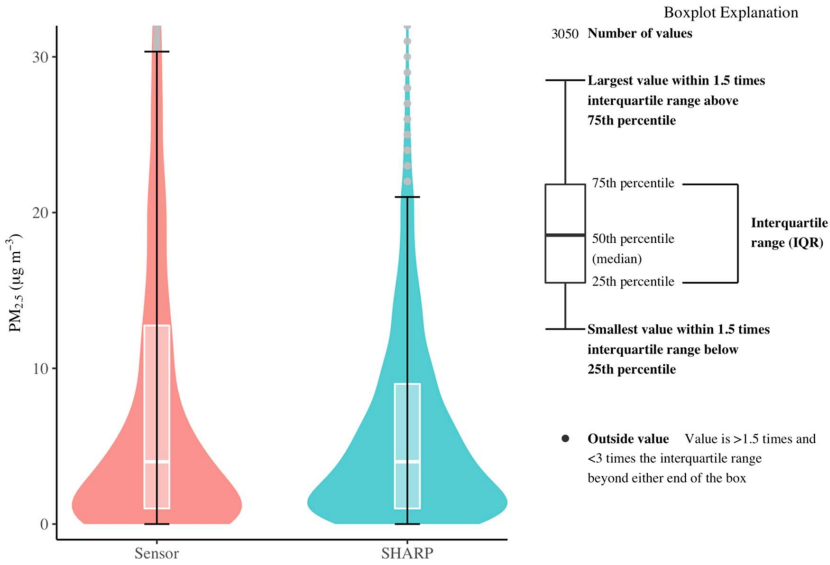
262 **3 Results and Discussion**

263 **3.1 Sensor evaluation**

264 **3.1.1 Hourly data**

265 The RMSE, MSE, and MAE between the low-cost sensor and SHARP for the hourly PM_{2.5} data were 10.58, 111.83, and
266 5.74. The Pearson correlation coefficient *r* value was 0.78. The PM_{2.5} concentrations by the sensor ranged from 0 µg m⁻³ to
267 178 µg m⁻³ with a standard deviation of 14.90 µg m⁻³ and a mean of 9.855 µg m⁻³. The PM_{2.5} concentrations by SHARP
268 ranged from 0 µg m⁻³ to 80 µg m⁻³ with a standard deviation of 7.80 and a mean of 6.55 µg m⁻³. Both SHARP and the low-
269 cost sensor dataset had a median of 4.00 µg m⁻³ based on hourly data (Fig. 43). The violin plot in Figure 4 describes the
270 distribution of the PM_{2.5} values measured by the low-cost sensor and SHARP using density curve. The width of each curve
271 represents the frequency of PM_{2.5} values at each concentration level. The p-value from the F-K test was less than 2.2×10⁻¹⁶,
272 indicating that the variance of the PM_{2.5} values measured by the low-cost sensor was statistically significantly different from
273 the variance of the PM_{2.5} values measured by the SHARP instrument.

274
275



276

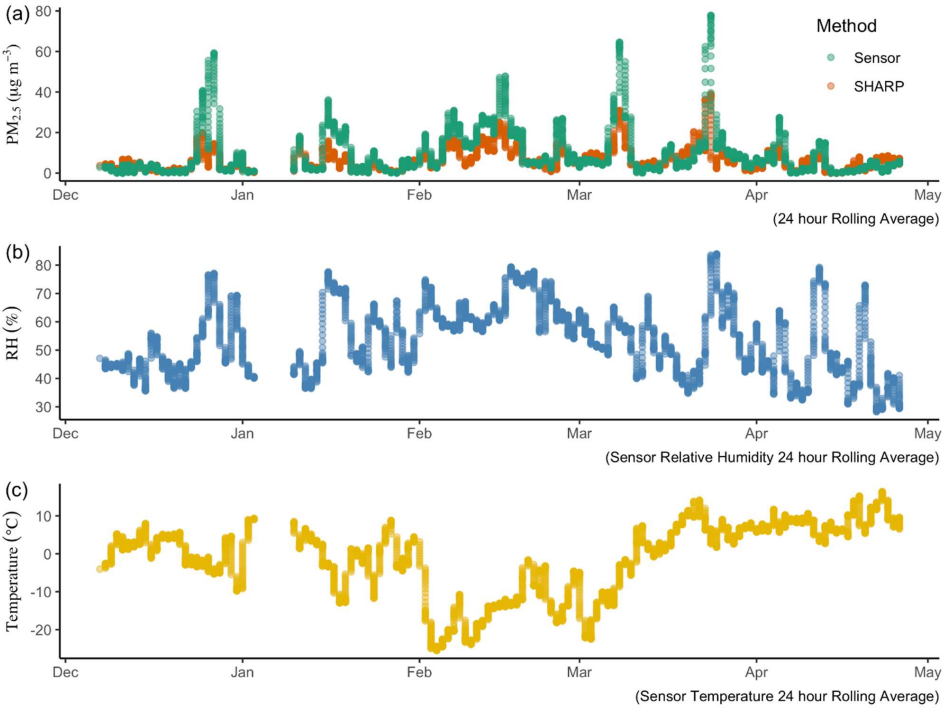
277 **Figure 43:** Comparison of the Hourly PM_{2.5} Values between the Low-Cost PM Sensor and SHARP. Based on 3,050 hourly paired data.
278 The low-cost sensor has 250 hourly data greater than 30 µg m⁻³. SHARP has 174 hourly data greater than 20 µg m⁻³. Bars indicate the 25th
279 and 75th percentile values, whiskers extend to values within 1.5 times IQR, and dots represent values outside of the IQR. The boxplot
280 explanation on the right is adjusted from DeCicco (2016)

Field Code Changed

281 **3.1.2 24 Hour rolling average data**

282 Over 24 hours, the median value for SHARP was 5.38 µg m⁻³ and for the low-cost sensor was 5.01 µg m⁻³. Over five months
283 (December 2018 to April 2019), the low-cost sensor tended to generate higher PM_{2.5} values compared to the SHARP
284 monitoring data (Fig. 54)

285



286
287 **Figure 54:** PM_{2.5}, Relative Humidity, and Temperature data on the basis of 24 hour rolling average

When $PM_{2.5}$ concentrations were greater than $10 \mu g m^{-3}$, the low-cost sensor consistently produced values that were higher than the reference method (Fig. 65). When the concentrations were less than $10 \mu g m^{-3}$, the performance of the low-cost sensor was closed to the reference method producing slightly smaller values (Fig. 65)

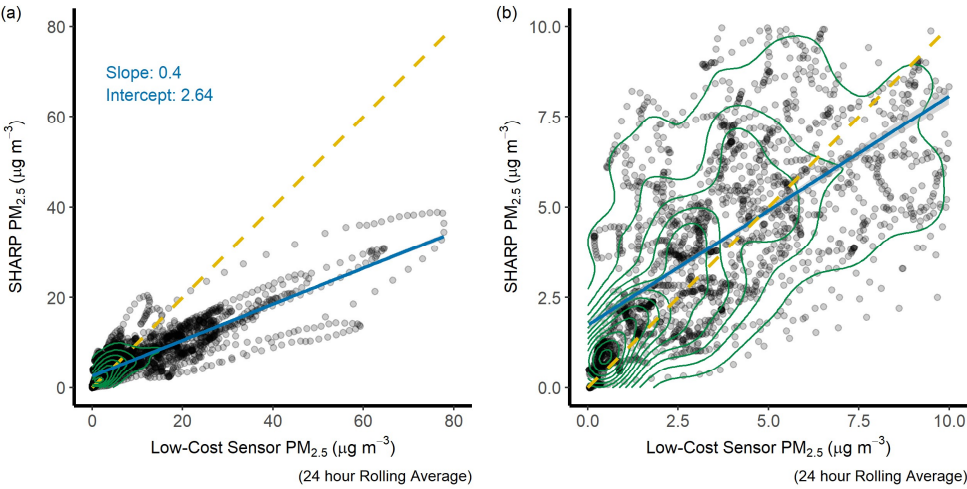


Figure 65: SHARP verse Low-Cost Sensor $PM_{2.5}$ Concentration ($\mu g m^{-3}$). The yellow dashed line is a 1:1 line. The solid blue line is a regression line. (a) plot is in full scale, (b) plot is a zoom-in plot of plot a. The green circle represents data density.

3.2 Calibration by simple linear regression and multiple linear regression

The RMSE was 4.91 calibrated by SLR and 4.65 by MLR (Table 2). The r value was 0.74 by the SLR and 0.77 by MLR . The p -values in the F-K test by the SLR and MRL were less than 0.05, which suggested that the variances of the $PM_{2.5}$ values were statistically significantly different.

Table 2: Calibration Results by SLR and MLR using Test Dataset

Criteria	Low-Cost Sensor	SLR	MLR
RMSE	9.93	4.91	4.65
MSE	98.62	24.09	21.61
MAE	5.63	3.21	3.09
Pearson r	0.74	0.74	0.77
p-value in the F-K test	7.062×10^{-09}	5.81×10^{-13}	9.90×10^{-10}
β_0	-	2.49	8.47

β_1	0.41	0.46
β_2		-0.12
β_3		-0.0055

300 Note: The test dataset contains 660 examples.

301 **3.3 Calibration by XGBoost**

302 The hyperparameters selected by the random search for the best model using XGBoost is presented in Table 3.

303 **Table 3: Hyperparameters for the Best XGBoost Model**

XGBoost Hyperparameters	Values
Number of trees to fit (n_estimator)	37
Maximum depth of a tree (max_depth)	9
Step size shrinkage used in update (learning_rate)	0.33
Subsample ratio of columns when constructing each tree (colsample_bytree)	0.83
Minimum loss reduction required to make a further partition on a leaf node of the tree (gamma)	6.36
L2 regularization (Ridge Regression) on weights (reg_lambda)	33.08
Minimum sum of instance weight needed in a child (min_child_weight)	25.53

304

305 In the training dataset, the RMSE was 3.03, and the MAE was 1.93 by the best XGBoost model. The RMSE in the test
306 dataset reduced by 57.8% using the XGBoost from 9.93 by the sensor to 4.19 (Table 4). The p-value in the F-K test using the
307 test dataset was 0.7256, which showed no evidence that the PM_{2.5} values varied with statistical significance between the
308 XGBoost predicted values and SHARP measured values.

309 **Table 4: Calibration Results by XGBoost using Test Dataset**

Criteria	Low-Cost Sensor	XGBoost
RMSE	9.93	4.19
MSE	98.62	17.61
MAE	5.63	2.63
Pearson r	0.74	0.82
p-value in the F-K test	7.062 ×10 ⁻⁰⁹	0.7256

310 Note: The test dataset contains 610 examples.

311 **3.4 Calibration by neural network**

312 The hyperparameters for the best NN model are presented in Table 5.

313 **Table 5: Hyperparameters for the Best Neural Network Model**

NN Hyperparameters	Values
--------------------	--------

Learning_rate	0.001
L2 regularization	0.01
Numbers of hidden layer(s)	5
Numbers of units in the hidden layer(s)	32-32-32-32-32
Optimization method	Nadam
Epochs	100

In the training dataset, the RMSE was 3.22, and the MAE was 2.17 by the best NN-based model. The RMSE reduced by 60% using the NN from 9.93 to 3.91 in the test dataset (Table 6). The p-value in the F-K test was 0.43, which suggested that the variances in the PM_{2.5} values were not statistically significantly different between the NN predicted values and SHARP measured values.

Table 6: Calibration Results by Neural Network using Test Dataset

Criteria	Low-Cost Sensor	Neural Network
RMSE	9.93	3.91
MSE	98.62	15.26
MAE	5.63	2.38
Pearson r	0.74	0.85
p-value in the F-K test	7.062×10^{-09}	0.43

Note: the test dataset includes 610 examples.

3.5 Discussion

3.5.1 Relative humidity impact

RH has significant effects on the low-cost sensor's responses. The RH trend matched the low-cost sensor's PM_{2.5} trend closely. The spikes in the low-cost sensor's PM_{2.5} trend corresponded with the increases of RH values, and the low-cost sensor intended to produce inaccurate high PM_{2.5} values when RH suddenly increased (Fig. 54). However, the relationship between PM_{2.5} and RH was not linear (Fig. 76)

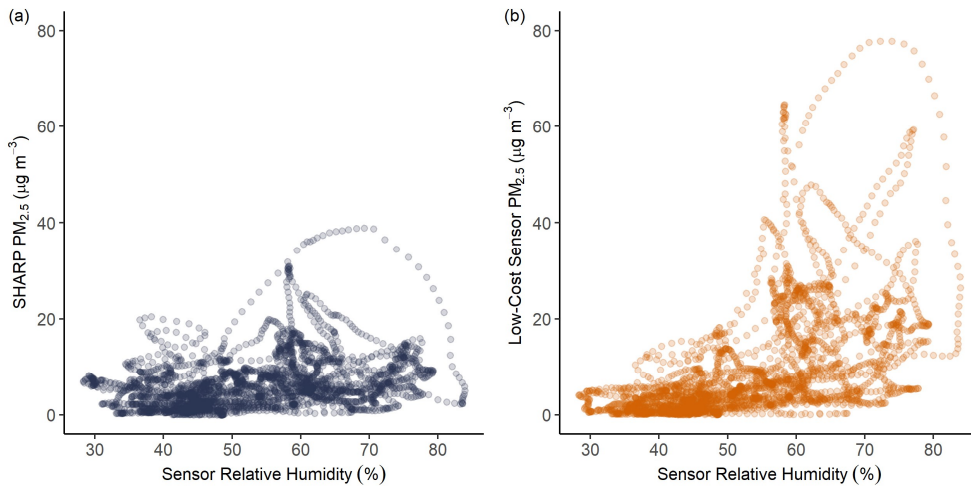


Figure 76: PM_{2.5} verse Relative Humidity

3.5.2 Seasonal impact

We assessed the seasonal impact on the low-cost sensor by comparing the mean of absolute differences of daily average between the sensor values and the SHARP values in winter (December 2018 to February 2019) and spring (March 2019 to April 2019). A descriptive statistics is presented in Table 7.

Table 7: Descriptive Statistics by Seasons

Season	Sample Size (n)	Mean ¹	Standard Deviation
Winter	78	5.13	6.95
Spring	57	4.76	6.45

Note: 1) Mean is calculated by $\sum_{i=1}^n (|sensor_{daily} - SHARP_{daily}|) / n$.

We used a two-sample t test to assess if the average differences for winter and spring were statistically significant. The p value of the t test was 0.754. Because $P = 0.754 > \alpha = 0.05$, we retained the null hypothesis. There was not sufficient evidence at the $\alpha = 0.05$ level to conclude that the means of absolute differences between the low-cost sensor and SHARP PM values were significantly different for winter season and spring season.

341
342

343 **3.5.32 Calibration assessment**

344 Descriptive statistics of the PM_{2.5} concentrations in the test dataset for SHARP, low-cost sensor, XGBoost, NN, SLR, and
345 MLR are presented in Table 87. The arithmetic mean of the PM_{2.5} concentrations measured by the low-cost sensor was
346 9.44 µg m⁻³. In contrast, the means of the PM_{2.5} concentrations were 6.44 µg m⁻³ by SHARP, 6.40 µg m⁻³ by XGBoost, and
347 6.09 µg m⁻³ by NN.

348 **Table 887:** Descriptive statistics of PM_{2.5} Concentrations using the Test Dataset

PM2.5 Concentration (µg m ⁻³)	SHARP	Low-Cost Sensor	XGBoost	NN	SLR	MLR
Minimum	0.00	0.00	0.00	0.19	2.49	0
1 st quartile	2.00	0.083	2.09	1.78	2.83	3.27
Median	4.00	4.00	4.98	4.16	4.13	4.79
Mean	6.44	9.44	6.40	6.09	6.37	6.42
3 rd quartile	8.00	11.94	8.61	8.20	7.39	7.18
Maximum	49.00	103.33	39.94	47.19	44.97	48.56
SD	7.32	13.53	6.03	6.23	5.57	5.67

349

350 NN and XGBoost produced data distributions that were similar to SHARP (Fig. 887). SLR had the worst performance.
351 Fig. 997 shows that SLR could not predict low concentrations. The predictions made by NN and XGBoost ranged from
352 0.19 µg m⁻³ to 47.19 µg m⁻³ and from 0.00 µg m⁻³ to 39.94 µg m⁻³.

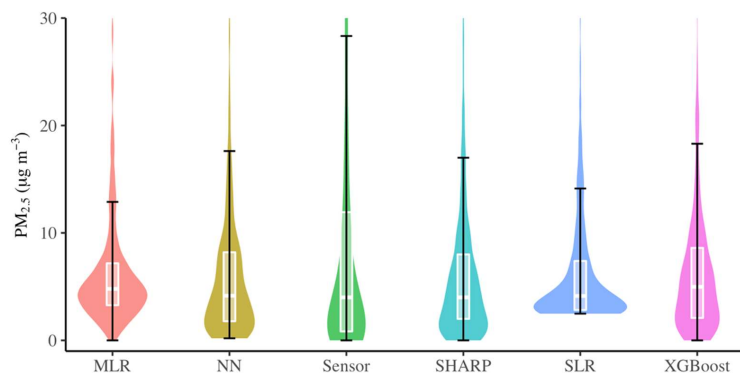


Figure 8: Data Density Comparison in the Test Dataset. Based on 610 Test Examples. NN: neural network, MRL: Multiple Linear Regression, SLR: Simple Linear Regression. $\text{PM}_{2.5}$ data greater than $30 \mu\text{g m}^{-3}$ are not shown in the figure. See the boxplot explanation in Figure 3.

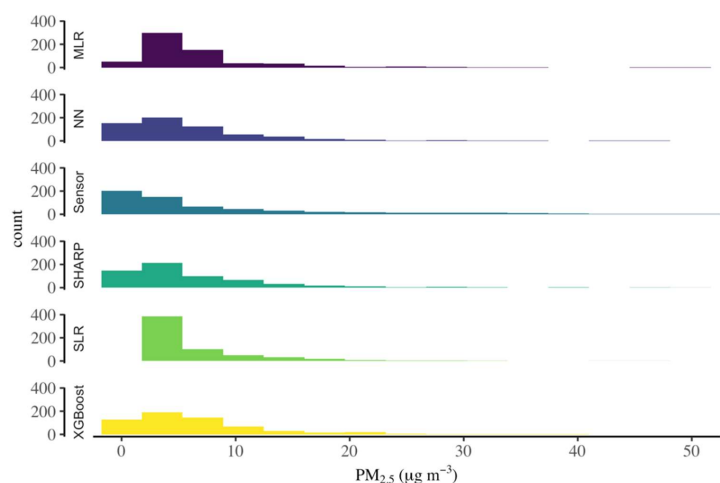
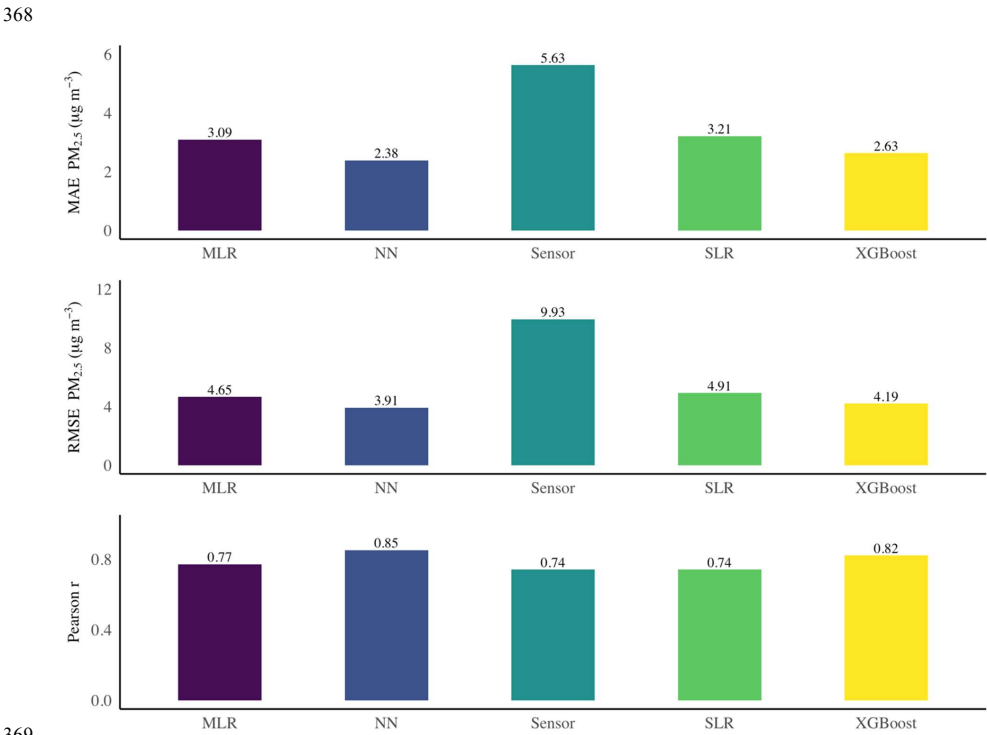


Figure 9: Data Distribution Comparison. Based on 610 Test Examples. NN: neural network, MRL: Multiple Linear Regression, SLR: Simple Linear Regression.

362
 363 In the test dataset, the NN produced the lowest MAE of 2.38 (Fig. 1009). The MAEs were 2.63 by XGBoost, 3.09 by
 364 MLR, and 3.21 by SLR, when compared with the PM_{2.5} data measured by the SHARP instrument. The NN also had the
 365 lowest RMSE score in the test dataset. The RMSEs were 3.91 for the NN, 4.19 for XGBoost, and 9.93 for the low-cost
 366 sensor (Fig. 1009). The Pearson r value by the NN was 0.85, compared to 0.74 by the low-cost sensor.



369
 370 **Figure 10:** Performances of Different Calibration Methods. Based on 610 Test Examples. NN: neural network, MRL: Multiple Linear
 371 Regression, SLR: Simple Linear Regression.

372 The XGBoost and NN machine learning algorithms have a better performance, compared to traditional SLR and MRL
 373 calibration methods. NN calibration reduced RMSE by 60%. Both NN and XGBoost demonstrated the ability to correct the
 374 bias for high concentrations made by the low-cost sensor (Fig. 1140 and Fig. 1224). Most of the values that were greater than

10 $\mu\text{g m}^{-3}$ in the NN model fall closer to the yellow 1:1 line (Fig. 11). NN had slightly better performance for low concentrations compared to XGBoost.

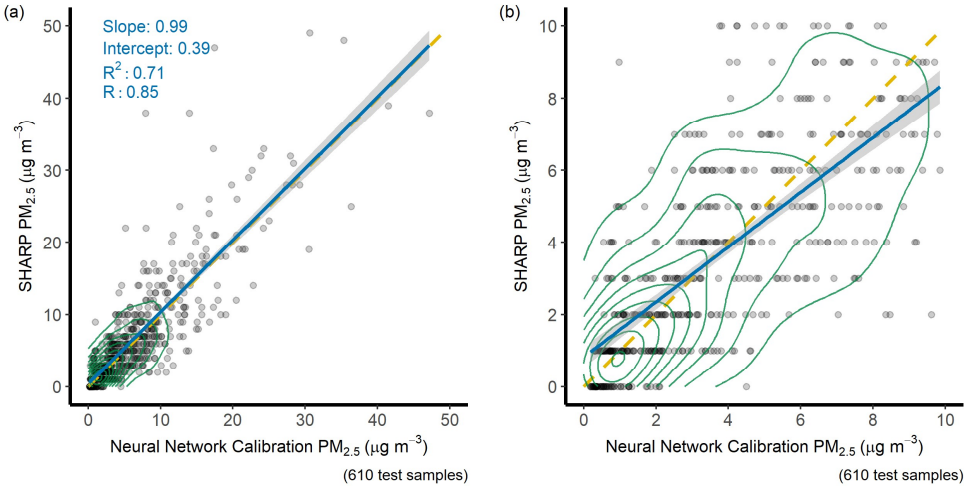
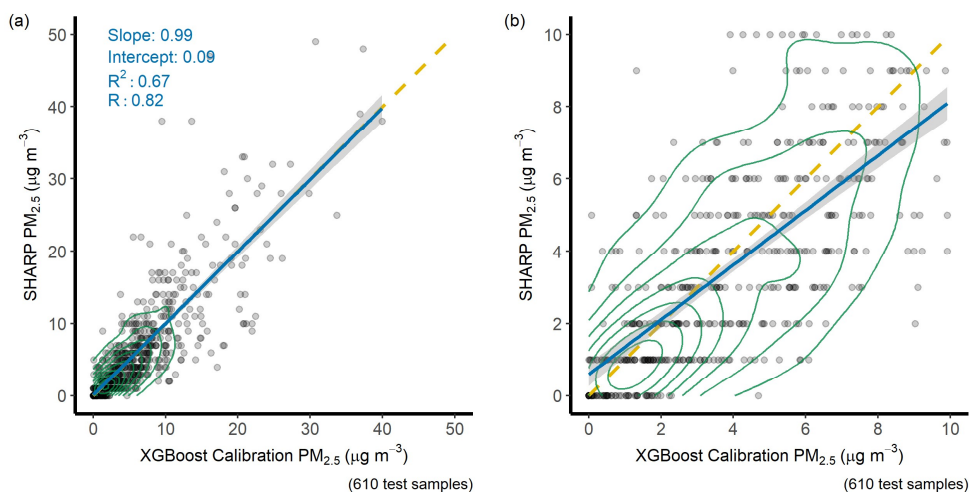


Figure 11: Comparison between the NN predictions and SHARP. Based on 610 test examples. Plot (a) is in full scale. Plot (b) is a zoom-in plot of plot (a). The solid blue line is a regression line. The yellow dashed line is a 1:1 line. The green circle represents data density. The grey area along the regression line represents 1 standard deviation.



381
 382 **Figure 12:** Comparison between the XGBoost predictions and SHARP. Based on 610 test examples. NN: Neural Network. Plot (a) is in
 383 full scale. Plot (b) is a zoom-in plot of plot (a). The solid blue line is a regression line. The yellow dashed line is a 1:1 line. The green
 384 circle represents data density. The grey area along the regression line represents 1 standard deviation.

385 4 Conclusions

386 In this study, we evaluated one low-cost sensor against a reference instrument – SHARP – using 3,050 hourly data from
 387 00:00 on December 7, 2018, to 23:00 on April 26, 2019. The p-value from the F-K test suggested that the variances in the
 388 $PM_{2.5}$ values were statistically significantly different between the low-cost sensor and the SHARP instrument. Based on the
 389 24-hour rolling average, the low-cost sensor in this study tended to report higher $PM_{2.5}$ values compared to the SHARP
 390 instrument. The low-cost sensor had strong bias when $PM_{2.5}$ concentrations were greater than $10 \mu g m^{-3}$. The study also
 391 showed that the sensor's bias responses are likely caused by the sudden changes of RH.

392 Four calibration methods were tested and compared, including SLR, MLR, NN, and XGBoost. The p-values from the
 393 F-K tests for the XGBoost and NN were greater than 0.05, which indicated that, after calibration by the XGBoost and the
 394 NN, the variances of the $PM_{2.5}$ values were not statistically significantly different from the variance of the $PM_{2.5}$ values
 395 measured by the SHARP instrument. In contrast, the p-values from the F-K tests for the SLR and MLR were still less than
 396 0.05. The NN generated the lowest RMSE score in the test dataset with 610 samples. The RMSE by NN was 3.91, the lowest
 397 of the four methods. RMSEs were 4.91 by SLP, 4.65 by MLR, and 4.19 by XGBoost.

398 However, a wide installation of low-cost sensors may still face challenges, including

- Durability of low-cost sensor. The low-cost sensor used in the study was deployed in ambient environment. We installed four sensors between December 7, 2018, and June 20, 2019. Only one sensor lasted approximately five months; the data from this sensor was used in this study. The other three sensors only lasted two weeks to one month and collected limited data. These three sensors did not collect enough data for machine learning and, therefore, were not used in this study.
- Missing data. In this study, the low-cost sensor dataset has 299 missing values for PM_{2.5} concentrations. The reason for the missing data is unknown.
- Transferability of machine learning models. The models, developed by the two more powerful machine learning algorithms and used to calibrate the low-cost sensor data, tend to be sensor-specific because of the nature of machine learning. Further research is needed to test the transferability of the models for broader use.

Data availability. The hourly sensor data and hourly SHARP data are provided online at [10.5281/zenodo.3473833](https://zenodo.org/record/3473833)

Author Contribution: MS conducted evaluation and calibrations. YX installed the sensor and monitored and collected the sensor data. MS and YX wrote the manuscript together and have equal contribution. SD edited the machine learning methods. DK secured the funding and supervised the project. All authors discussed the results and commented on the manuscript.

Competing interests. The authors declare no competing interest.

Disclaimer. Reference to any companies or specific commercial products does not constitute endorsement or recommendation by the authors.

Acknowledgments. The authors wish to thank SensorUp for providing the low-cost sensors, and Calgary Region Airshed Zone's air quality program manager Mandeep Dhaliwal for helping with the installation of the PM sensors and a 4G LTE router, as well as the collection of the SHARP data. The authors would also like to thank Jessica Coles for editing this manuscript.

430 The project was funded by Natural Sciences and Engineering Research Council of Canada (NSERC) Engage Program (No.
431 EGP 521823–17) and NSERC Collaborative Research and Development Program (No. CRDPJ 535813-18).

432 **References**

433 [Bergstra, J. and Bengio, Y.: Random Search for Hyper-Parameter Optimization, J. Mach. Learn. Res., 13, 281–305, 2012.](#)

434 [CDNova Instrument Ltd.: SHARP Cost Estimate, 2017.](#)

435 [Charlson, R. J., Schwartz, S. E., Hales, J. M., Cess, R. D., Coakley, J. A., Hansen, J. E. and Hofmann, D. J.: Climate Forcing](#)
436 [by Anthropogenic Aerosols, Science, 255\(5043\), 423–430, doi:10.1126/science.255.5043.423, 1992.](#)

437 [Chen, T. and Guestrin, C.: XGBoost: A Scalable Tree Boosting System, in Proceedings of the 22nd ACM SIGKDD](#)
438 [International Conference on Knowledge Discovery and Data Mining - KDD '16, pp. 785–794, ACM Press, San Francisco,](#)
439 [California, USA., 2016.](#)

440 [Chong, C.-Y. and Kumar, S. P.: Sensor networks: Evolution, opportunities, and challenges, Proc. IEEE, 91\(8\), 1247–1256,](#)
441 [doi:10.1109/JPROC.2003.814918, 2003.](#)

442 [Chow, J. C. and Watson, J. G.: Guideline on Speciated Particulate Monitoring, \[online\] Available from:](#)
443 <https://www3.epa.gov/ttn/amtic/files/ambient/pm25/spec/driscpec.pdf>, 1998.

444 [Conover, W. J., Johnson, M. E. and Johnson, M. M.: A Comparative Study of Tests for Homogeneity of Variances, with](#)
445 [Applications to the Outer Continental Shelf Bidding Data., 1981.](#)

446 [Cordero, J. M., Borge, R. and Narros, A.: Using statistical methods to carry out in field calibrations of low cost air quality](#)
447 [sensors, Sens. Actuators B Chem., 267, 245–254, doi:10.1016/j.snb.2018.04.021, 2018.](#)

448 [De Vito, S., Massera, E., Piga, M., Martinotto, L. and Di Francia, G.: On field calibration of an electronic nose for benzene](#)
449 [estimation in an urban pollution monitoring scenario, Sens. Actuators B Chem., 129\(2\), 750–757,](#)
450 [doi:10.1016/j.snb.2007.09.060, 2008.](#)

451 [De Vito, S., Piga, M., Martinotto, L. and Di Francia, G.: CO, NO2 and NOx urban pollution monitoring with on-field](#)
452 [calibrated electronic nose by automatic bayesian regularization, Sens. Actuators B Chem., 143\(1\), 182–191,](#)
453 [doi:10.1016/j.snb.2009.08.041, 2009.](#)

454 [De Vito, S., Esposito, E., Salvato, M., Popoola, O., Formisano, F., Jones, R. and Di Francia, G.: Calibrating chemical](#)
455 [multisensory devices for real world applications: An in-depth comparison of quantitative machine learning approaches, Sens.](#)
456 [Actuators B Chem., 255, 1191–1210, doi:10.1016/j.snb.2017.07.155, 2018.](#)

457 [DeCicco, L.: Exploring ggplot2 boxplots - Defining limits and adjusting style, Explor. Ggplot2 Boxplots - Defin. Limits](#)
458 [Adjust. Style \[online\] Available from: https://owi.usgs.gov/blog/boxplots/, 2016.](#)

459 [Esposito, E., De Vito, S., Salvato, M., Bright, V., Jones, R. L. and Popoola, O.: Dynamic neural network architectures for on](#)
460 [field stochastic calibration of indicative low cost air quality sensing systems, Sens. Actuators B Chem., 231, 701–713,](#)
461 [doi:10.1016/j.snb.2016.03.038, 2016.](#)

Formatted: Bibliography, Automatically adjust right indent when grid is defined, Widow/Orphan control, Adjust space between Latin and Asian text, Adjust space between Asian text and numbers

462 [Fligner, M. A. and Killeen, T. J.: Distribution-Free Two-Sample Tests for Scale, J. Am. Stat. Assoc., 71\(353\), 210–213,](#)
463 [doi:10.1080/01621459.1976.10481517, 1976.](#)

464 [Government of Canada: National Air Pollution Surveillance \(NAPS\) Network - Open Government Portal, Natl. Air Pollut.](#)
465 [Surveill. NAPS Netw. \[online\] Available from: \[https://open.canada.ca/data/en/dataset/1b36a356-defd-4813-acea-\]\(https://open.canada.ca/data/en/dataset/1b36a356-defd-4813-acea-47bc3abd859b\)](#)
466 [47bc3abd859b \(Accessed 17 September 2019\), 2019.](#)

467 [Holstius, D. M., Pillarisetti, A., Smith, K. R. and Seto, E.: Field calibrations of a low-cost aerosol sensor at a regulatory](#)
468 [monitoring site in California, Atmospheric Meas. Tech., 7\(4\), 1121–1131, doi:10.5194/amt-7-1121-2014, 2014.](#)

469 [Jayaratne, R., Liu, X., Thai, P., Dunbabin, M. and Morawska, L.: The influence of humidity on the performance of a low-](#)
470 [cost air particle mass sensor and the effect of atmospheric fog, Atmospheric Meas. Tech., 11\(8\), 4883–4890,](#)
471 [doi:10.5194/amt-11-4883-2018, 2018.](#)

472 [Krizhevsky, A., Sutskever, I. and Hinton, G. E.: ImageNet classification with deep convolutional neural networks, Commun](#)
473 [ACM, 60\(6\), 84–90, 2017.](#)

474 [Kumar, P., Morawska, L., Martani, C., Biskos, G., Neophytou, M., Di Sabatino, S., Bell, M., Norford, L. and Britter, R.: The](#)
475 [rise of low-cost sensing for managing air pollution in cities, Environ. Int., 75, 199–205, doi:10.1016/j.envint.2014.11.019,](#)
476 [2015.](#)

477 [Laerd Statistics: Spearman's Rank-Order Correlation - A guide to when to use it, what it does and what the assumptions are.,](#)
478 [Laerd Stat. \[online\] Available from: \[https://statistics.laerd.com/statistical-guides/spearmans-rank-order-correlation-\]\(https://statistics.laerd.com/statistical-guides/spearmans-rank-order-correlation-statistical-guide.php\)](#)
479 [statistical-guide.php \(Accessed 24 February 2020\), 2020.](#)

480 [LeCun, Y., Bengio, Y. and Hinton, G.: Deep learning, Nature, 521\(7553\), 436–444, doi:10.1038/nature14539, 2015.](#)

481 [Lewis, A. C., Lee, J. D., Edwards, P. M., Shaw, M. D., Evans, M. J., Moller, S. J., Smith, K. R., Buckley, J. W., Ellis, M.,](#)
482 [Gillot, S. R. and White, A.: Evaluating the performance of low cost chemical sensors for air pollution research, Faraday](#)
483 [Discuss., 189, 85–103, doi:10.1039/C5FD00201J, 2016.](#)

484 [Lin, Y., Dong, W. and Chen, Y.: Calibrating Low-Cost Sensors by a Two-Phase Learning Approach for Urban Air Quality](#)
485 [Measurement, Proc. ACM Interact. Mob. Wearable Ubiquitous Technol., 2\(1\), 1–18, doi:10.1145/3191750, 2018.](#)

486 [Loh, B. G. and Choi, G.-H.: Calibration of Portable Particulate Matter-Monitoring Device using Web Query and Machine](#)
487 [Learning, Saf. Health Work, S2093791119302811, doi:10.1016/j.shaw.2019.08.002, 2019.](#)

488 [Maag, B., Zhou, Z. and Thiele, L.: A Survey on Sensor Calibration in Air Pollution Monitoring Deployments, IEEE Internet](#)
489 [Things J., 5\(6\), 4857–4870, doi:10.1109/IIOT.2018.2853660, 2018.](#)

490 [Myers, L. and Sirois, M. J.: Spearman Correlation Coefficients, Differences between, in Encyclopedia of Statistical](#)
491 [Sciences, edited by S. Kotz, C. B. Read, N. Balakrishnan, B. Vidakovic, and N. L. Johnson, p. ess5050.pub2, John Wiley &](#)
492 [Sons, Inc., Hoboken, NJ, USA., 2006.](#)

493 [Papapostolou, V., Zhang, H., Feenstra, B. J. and Polidori, A.: Development of an environmental chamber for evaluating the](#)
494 [performance of low-cost air quality sensors under controlled conditions, Atmos. Environ., 171, 82–90,](#)
495 [doi:10.1016/j.atmosenv.2017.10.003, 2017.](#)

496 Patashnick, H. and Rupprecht, E. G.: Continuous PM-10 Measurements Using the Tapered Element Oscillating
497 Microbalance, *J. Air Waste Manag. Assoc.*, 41(8), 1079–1083, doi:10.1080/10473289.1991.10466903, 1991.

498 RStudio: Why Use Keras?, [online] Available from: https://keras.rstudio.com/articles/why_use_keras.html, 2018.

499 Rumelhart, D. E., Hinton, G. E. and Williams, R. J.: Learning representations by back-propagating errors, *Nature*,
500 323(6088), 533–536, doi:10.1038/323533a0, 1986.

501 Seinfeld, J. H. and Pandis, S. N.: Atmospheric chemistry and physics: from air pollution to climate change, Wiley, New
502 York., 1998.

503 Si, M., Tarnoczi, T. J., Wiens, B. M. and Du, K.: Development of Predictive Emissions Monitoring System Using Open
504 Source Machine Learning Library – Keras: A Case Study on a Cogeneration Unit, *IEEE Access*, 7, 113463–113475,
505 doi:10.1109/ACCESS.2019.2930555, 2019.

506 de Smith, M.: Statistical Analysis Handbook, 2018 Edition., The Winchelsea Press, Drumlin Security Ltd, Edinburgh.
507 [online] Available from: http://www.statsref.com/HTML/index.html?fligner-killeen_test.html, 2018.

508 Snyder, E. G., Watkins, T. H., Solomon, P. A., Thoma, E. D., Williams, R. W., Hagler, G. S. W., Shelow, D., Hindin, D. A.,
509 Kilaru, V. J. and Preuss, P. W.: The Changing Paradigm of Air Pollution Monitoring, *Environ. Sci. Technol.*, 47(20), 11369–
510 11377, doi:10.1021/es4022602, 2013.

511 Spinelle, L., Gerboles, M., Villani, M. G., Aleixandre, M. and Bonavitacola, F.: Field calibration of a cluster of low-cost
512 available sensors for air quality monitoring. Part A: Ozone and nitrogen dioxide, *Sens. Actuators B Chem.*, 215, 249–257,
513 doi:10.1016/j.snb.2015.03.031, 2015.

514 Spinelle, L., Gerboles, M., Villani, M. G., Aleixandre, M. and Bonavitacola, F.: Field calibration of a cluster of low-cost
515 commercially available sensors for air quality monitoring. Part B: NO, CO and CO₂, *Sens. Actuators B Chem.*, 238, 706–
516 715, doi:10.1016/j.snb.2016.07.036, 2017.

517 Timbers, F.: Random Search for Hyper-Parameter Optimization | Finbarr Timbers, [online] Available from:
518 <https://finbarr.ca/random-search-hyper-parameter-optimization/> (Accessed 4 October 2019), 2017.

519 US EPA: LIST OF DESIGNATED REFERENCE AND EQUIVALENT METHODS, [online] Available from:
520 <https://www3.epa.gov/ttnamti1/files/ambient/criteria/AMTIC%20List%20Dec%202016-2.pdf> (Accessed 7 October 2019),
521 2016.

522 Wang, Y., Li, J., Jing, H., Zhang, Q., Jiang, J. and Biswas, P.: Laboratory Evaluation and Calibration of Three Low-Cost
523 Particle Sensors for Particulate Matter Measurement, *Aerosol Sci. Technol.*, 49(11), 1063–1077,
524 doi:10.1080/02786826.2015.1100710, 2015.

525 White, R., Paprotny, I., Doering, F., Cascio, W., Solomon, P. and Gundel, L.: Sensors and “apps” for community-based:
526 Atmospheric monitoring, *EM Air Waste Manag. Assoc. Mag. Environ. Manag.*, 36–40, 2012.

527 Williams, R., Kaufman, A., Hanley, T., Rice, J. and Garvey, S.: Evaluation of Field-deployed Low Cost PM Sensors, U.S.
528 Environmental Protection Agency., [online] Available from:
529 https://cfpub.epa.gov/si/si_public_record_report.cfm?Lab=NREL&DirEntryId=297517 (Accessed 17 September 2019),
530 2014.

de Winter, J. C. F., Gosling, S. D. and Potter, J.: Comparing the Pearson and Spearman correlation coefficients across distributions and sample sizes: A tutorial using simulations and empirical data., *Psychol. Methods*, 21(3), 273–290, doi:10.1037/met0000079, 2016.

XGBoost developers: XGBoost Parameters — xgboost 1.0.0-SNAPSHOT documentation, [online] Available from: <https://xgboost.readthedocs.io/en/latest/parameter.html> (Accessed 24 January 2020), 2019.

Xiong, Y., Zhou, J., Schauer, J. J., Yu, W. and Hu, Y.: Seasonal and spatial differences in source contributions to PM_{2.5} in Wuhan, China, *Sci. Total Environ.*, 577, 155–165, doi:10.1016/j.scitotenv.2016.10.150, 2017.

Zheng, A.: Evaluating Machine Learning Models, First Edition., O'Reilly Media, Inc., 1005 Gravenstein Highway North, Sebastopol, CA., 2015.

Zheng, T., Bergin, M. H., Johnson, K. K., Tripathi, S. N., Shirodkar, S., Landis, M. S., Sutaria, R. and Carlson, D. E.: Field evaluation of low-cost particulate matter sensors in high- and low-concentration environments, *Atmospheric Meas. Tech.*, 11(8), 4823–4846, doi:10.5194/amt-11-4823-2018, 2018.

Zikova, N., Hopke, P. K. and Ferro, A. R.: Evaluation of new low-cost particle monitors for PM_{2.5} concentrations measurements, *J. Aerosol Sci.*, 105, 24–34, doi:10.1016/j.jaerosci.2016.11.010, 2017.

Zimmerman, N., Presto, A. A., Kumar, S. P. N., Gu, J., Haurlyliuk, A., Robinson, E. S., Robinson, A. L. and R. Subramanian: A machine learning calibration model using random forests to improve sensor performance for lower-cost air quality monitoring, *Atmospheric Meas. Tech.*, 11(1), 291–313, doi:10.5194/amt-11-291-2018, 2018.

Bergstra, J. and Bengio, Y.: Random Search for Hyper-Parameter Optimization, *J. Mach. Learn. Res.*, 13, 281–305, 2012.

CDNova Instrument Ltd.: SHARP Cost Estimate, 2017.

Charlson, R. J., Schwartz, S. E., Hales, J. M., Cess, R. D., Coakley, J. A., Hansen, J. E. and Hofmann, D. J.: Climate Forcing by Anthropogenic Aerosols, *Science*, 255(5043), 423–430, doi:10.1126/science.255.5043.423, 1992.

Chen, T. and Guestrin, C.: XGBoost: A Scalable Tree Boosting System, in *Proceedings of the 22nd ACM SIGKDD International Conference on Knowledge Discovery and Data Mining – KDD '16*, pp. 785–794, ACM Press, San Francisco, California, USA., 2016.

Chong, C.-Y. and Kumar, S. P.: Sensor networks: Evolution, opportunities, and challenges, *Proc. IEEE*, 91(8), 1247–1256, doi:10.1109/JPROC.2003.814918, 2003.

Chow, J. C. and Watson, J. G.: Guideline on Speciated Particulate Monitoring, [online] Available from: <https://www3.epa.gov/ttn/amt/c/files/ambient/pm25/spec/drisspec.pdf>, 1998.

Conover, W. J., Johnson, M. E. and Johnson, M. M.: A Comparative Study of Tests for Homogeneity of Variances, with Applications to the Outer Continental Shelf Bidding Data., 1981.

Cordero, J. M., Borge, R. and Narros, A.: Using statistical methods to carry out in-field calibrations of low-cost air quality sensors, *Sens. Actuators B-Chem.*, 267, 245–254, doi:10.1016/j.snb.2018.04.021, 2018.

De Vito, S., Massera, E., Piga, M., Martinotto, L. and Di Francia, G.: On field calibration of an electronic nose for benzene estimation in an urban pollution monitoring scenario, *Sens. Actuators B Chem.*, 129(2), 750–757, doi:10.1016/j.snb.2007.09.060, 2008.

De Vito, S., Piga, M., Martinotto, L. and Di Francia, G.: CO, NO₂, and NO_x urban pollution monitoring with on-field calibrated electronic nose by automatic bayesian regularization, *Sens. Actuators B Chem.*, 143(1), 182–191, doi:10.1016/j.snb.2009.08.041, 2009.

De Vito, S., Esposito, E., Salvato, M., Popoola, O., Formisano, F., Jones, R. and Di Francia, G.: Calibrating chemical multisensory devices for real world applications: An in-depth comparison of quantitative machine learning approaches, *Sens. Actuators B Chem.*, 255, 1191–1210, doi:10.1016/j.snb.2017.07.155, 2018.

DeCicco, L.: Exploring ggplot2 boxplots – Defining limits and adjusting style, *Explor. Ggplot2 Boxplots – Defin. Limits Adjust. Style* [online]. Available from: <https://owi.usgs.gov/blog/boxplots/>, 2016.

Esposito, E., De Vito, S., Salvato, M., Bright, V., Jones, R. L. and Popoola, O.: Dynamic neural network architectures for on field stochastic calibration of indicative low cost air quality sensing systems, *Sens. Actuators B Chem.*, 231, 701–713, doi:10.1016/j.snb.2016.03.038, 2016.

Fligner, M. A. and Killeen, T. J.: Distribution-Free Two-Sample Tests for Scale, *J. Am. Stat. Assoc.*, 71(353), 210–213, doi:10.1080/01621459.1976.10481517, 1976.

Government of Canada: National Air Pollution Surveillance (NAPS) Network – Open Government Portal, *Natl. Air Pollut. Surveill. NAPS Netw.* [online]. Available from: <https://open.canada.ca/data/en/dataset/1b36a356-defd-4813-acea-47be3abd859b> (Accessed 17 September 2019), 2019.

Holstius, D. M., Pillarisetti, A., Smith, K. R. and Seto, E.: Field calibrations of a low-cost aerosol sensor at a regulatory monitoring site in California, *Atmospheric Meas. Tech.*, 7(4), 1121–1131, doi:10.5194/amt-7-1121-2014, 2014.

Jayarathne, R., Liu, X., Thai, P., Dunbabin, M. and Morawska, L.: The influence of humidity on the performance of a low-cost air particle mass sensor and the effect of atmospheric fog, *Atmospheric Meas. Tech.*, 11(8), 4883–4890, doi:10.5194/amt-11-4883-2018, 2018.

Krizhevsky, A., Sutskever, I. and Hinton, G. E.: ImageNet classification with deep convolutional neural networks, *Commun ACM*, 60(6), 84–90, 2017.

Kumar, P., Morawska, L., Martani, C., Biskos, G., Neophytou, M., Di Sabatino, S., Bell, M., Norford, L. and Britter, R.: The rise of low-cost sensing for managing air pollution in cities, *Environ. Int.*, 75, 199–205, doi:10.1016/j.envint.2014.11.019, 2015.

LeCun, Y., Bengio, Y. and Hinton, G.: Deep learning, *Nature*, 521(7553), 436–444, doi:10.1038/nature14539, 2015.

Lewis, A. C., Lee, J. D., Edwards, P. M., Shaw, M. D., Evans, M. J., Moller, S. J., Smith, K. R., Buckley, J. W., Ellis, M., Gillot, S. R. and White, A.: Evaluating the performance of low-cost chemical sensors for air pollution research, *Faraday Discuss.*, 189, 85–103, doi:10.1039/C5FD00201J, 2016.

Lin, Y., Dong, W. and Chen, Y.: Calibrating Low-Cost Sensors by a Two-Phase Learning Approach for Urban Air Quality Measurement, *Proc. ACM Interact. Mob. Wearable Ubiquitous Technol.*, 2(1), 1–18, doi:10.1145/3191750, 2018.

598 Loh, B. G. and Choi, G. H.: Calibration of Portable Particulate Matter Monitoring Device using Web Query and Machine
599 Learning, *Saf. Health Work*, S2093791119302811, doi:10.1016/j.shaw.2019.08.002, 2019.

600 Maag, B., Zhou, Z. and Thiele, L.: A Survey on Sensor Calibration in Air Pollution Monitoring Deployments, *IEEE Internet*
601 *Things J.*, 5(6), 4857–4870, doi:10.1109/IOT.2018.2853660, 2018.

602 Papapostolou, V., Zhang, H., Feenstra, B. J. and Polidori, A.: Development of an environmental chamber for evaluating the
603 performance of low-cost air quality sensors under controlled conditions, *Atmos. Environ.*, 171, 82–90,
604 doi:10.1016/j.atmosenv.2017.10.003, 2017.

605 Patashnick, H. and Rupprecht, E. G.: Continuous PM₁₀ Measurements Using the Tapered Element Oscillating
606 Microbalance, *J. Air Waste Manag. Assoc.*, 41(8), 1079–1083, doi:10.1080/10473289.1991.10466903, 1991.

607 RStudio: Why Use Keras?, [online] Available from: https://keras.rstudio.com/articles/why_use_keras.html, 2018.

608 Rumelhart, D. E., Hinton, G. E. and Williams, R. J.: Learning representations by back-propagating errors, *Nature*,
609 323(6088), 533–536, doi:10.1038/323533a0, 1986.

610 Seinfeld, J. H. and Pandis, S. N.: *Atmospheric chemistry and physics: from air pollution to climate change*, Wiley, New
611 York, 1998.

612 Si, M., Tarnoezi, T. J., Wiens, B. M. and Du, K.: Development of Predictive Emissions Monitoring System Using Open
613 Source Machine Learning Library — Keras: A Case Study on a Cogeneration Unit, *IEEE Access*, 7, 113463–113475,
614 doi:10.1109/ACCESS.2019.2930555, 2019.

615 de Smith, M.: *Statistical Analysis Handbook*, 2018 Edition., The Winchelsea Press, Drumlin Security Ltd, Edinburgh.
616 [online] Available from: http://www.statsref.com/HTML/index.html?fligner-killeen_test.html, 2018.

617 Snyder, E. G., Watkins, T. H., Solomon, P. A., Thoma, E. D., Williams, R. W., Hagler, G. S. W., Shelow, D., Hindin, D. A.,
618 Kilaru, V. J. and Preuss, P. W.: The Changing Paradigm of Air Pollution Monitoring, *Environ. Sci. Technol.*, 47(20), 11369–
619 11377, doi:10.1021/es4022602, 2013.

620 Spinelle, L., Gerboles, M., Villani, M. G., Aleixandre, M. and Bonavitacola, F.: Field calibration of a cluster of low-cost
621 available sensors for air quality monitoring. Part A: Ozone and nitrogen dioxide, *Sens. Actuators B-Chem.*, 215, 249–257,
622 doi:10.1016/j.snb.2015.03.031, 2015.

623 Spinelle, L., Gerboles, M., Villani, M. G., Aleixandre, M. and Bonavitacola, F.: Field calibration of a cluster of low-cost
624 commercially available sensors for air quality monitoring. Part B: NO, CO, and CO₂, *Sens. Actuators B-Chem.*, 238, 706–
625 715, doi:10.1016/j.snb.2016.07.036, 2017.

626 Timbers, F.: Random Search for Hyper-Parameter Optimization | Finbarr Timbers, [online] Available from:
627 <https://finbarr.ca/random-search-hyper-parameter-optimization/> (Accessed 4 October 2019), 2017.

628 US EPA: LIST OF DESIGNATED REFERENCE AND EQUIVALENT METHODS, [online] Available from:
629 <https://www3.epa.gov/ttnamti1/files/ambient/criteria/AMTIC%20List%20Dec%202016-2.pdf> (Accessed 7 October 2019),
630 2016.

631 Wang, Y., Li, J., Jing, H., Zhang, Q., Jiang, J. and Biswas, P.: Laboratory Evaluation and Calibration of Three Low-Cost
632 Particle Sensors for Particulate Matter Measurement, *Aerosol Sci. Technol.*, 49(11), 1063–1077,
633 doi:10.1080/02786826.2015.1100710, 2015.

634 White, R., Paprotny, I., Doering, F., Cascio, W., Solomon, P. and Gundel, L.: Sensors and “apps” for community-based:
635 Atmospheric monitoring, *EM Air Waste Manag. Assoc. Mag. Environ. Manag.*, 36–40, 2012.

636 Williams, R., Kaufman, A., Hanley, T., Rice, J. and Garvey, S.: Evaluation of Field-deployed Low-Cost PM Sensors, U.S.
637 Environmental Protection Agency, [online] Available from:
638 https://cfpub.epa.gov/si/si_public_record_report.cfm?Lab=NERL&DirEntryId=297517 (Accessed 17 September 2019),
639 2014.

640 Xiong, Y., Zhou, J., Schauer, J. J., Yu, W. and Hu, Y.: Seasonal and spatial differences in source contributions to PM_{2.5} in
641 Wuhan, China, *Sci. Total Environ.*, 577, 155–165, doi:10.1016/j.scitotenv.2016.10.150, 2017.

642 Zheng, T., Bergin, M. H., Johnson, K. K., Tripathi, S. N., Shirodkar, S., Landis, M. S., Sutaria, R. and Carlson, D. E.: Field
643 evaluation of low-cost particulate matter sensors in high- and low-concentration environments, *Atmospheric Meas. Tech.*,
644 11(8), 4823–4846, doi:10.5194/amt-11-4823-2018, 2018.

645 Zikova, N., Hopke, P. K. and Ferro, A. R.: Evaluation of new low-cost particle monitors for PM_{2.5} concentrations
646 measurements, *J. Aerosol Sci.*, 105, 24–34, doi:10.1016/j.jaerosci.2016.11.010, 2017.

647 Zimmerman, N., Presto, A. A., Kumar, S. P. N., Gu, J., Hauryliuk, A., Robinson, E. S., Robinson, A. L. and R.
648 Subramanian: A machine learning calibration model using random forests to improve sensor performance for lower-cost air
649 quality monitoring, *Atmospheric Meas. Tech.*, 11(1), 291–313, doi:10.5194/amt-11-291-2018, 2018.

650